Available online at www.sciencedirect.com

ScienceDirect

Ciência & Tecnologia dos Materiais 29 (2017) e65–e70

http://ees.elsevier.com/ctmat

Special Issue "Materiais 2015"

Upward and downward unsteady-state directional solidification of a hypoeutectic Al-3wt.%Mg alloy

C. Brito[a, *], F. Bertelli[f], M.A.P. Castanho[c], P.R. Goulart[d], N. Cheung[b], J.E. Spinelli[e], A. Garcia[b]

[a]*Department of Marine Sciences, Federal University of São Paulo, UNIFESP, Santos, SP, Brazil*
[b]*Department of Manufacturing and Materials Engineering, University of Campinas, UNICAMP, Campinas, SP, Brazil*
[c]*Institute for Technological Research, IPT, São Paulo, SP, Brazil*
[d]*Federal Institute of Education, Science and Technology of São Paulo, IFSP, Itapetininga, SP, Brazil*
[e]*Department of Materials Engineering, Federal University of São Carlos, UFSCar, São Carlos, SP, Brazil*
[f]*Postgraduate Program of Mechanical Engineering, Santa Cecília University, UNISANTA, Santos, SP, Brazil*

Abstract

Solidification thermal parameters, such as growth rate, cooling rate and dendrite arm spacing (λ), have been measured in a hypoeutectic Al-Mg alloy directionally solidified under upward and downward transient heat flow conditions. The experimental setup used in this work consists of a water-cooled mould with heat being extracted from the bottom or the top, promoting upward and downward directional solidification, respectively. It is shown that the dendritic arm spacing are not significantly affected by interdendritic convection for both solidification configurations and single growth laws are proposed for both cases. The Bouchard-Kirkaldy model is shown to overestimate the experimental primary dendritic arm spacing, despite fitting properly the secondary dendrite arm spacing.

Keywords: Directional solidification; microstructure; convection; Al-Mg alloy.

1. Introduction

Al-Mg alloys are important for engineering applications in the automotive, aeronautical industries and in the manufacture of marine components [1]. Magnesium has been largely added to aluminum alloys in order to increase mechanical and corrosion resistances [1,2]. The solidification process encompasses heat transfer, fluid flow and solute transport mechanisms, which in turn influence the development of the microstructure, affecting the phases' morphology, their scale and distribution [3,4]. Studies on the effects of the direction of heat extraction (downward or upward) during solidification of metallic alloys are scarce in the literature, mainly under unsteady state conditions. Among the few studies concerning such heat flow conditions, the investigations by Burden and Hunt [5], Spinelli *et al.* [6], Spinelli *et al.* [7], Spinelli *et al.* [8] and Wang *et al.* [9] may be cited.

Burden and Hunt [5] have carried out experiments with non-metallic alloys (NH_4Cl/H_2O) in order to investigate the effect of downward and upward solidification on the dendritic growth of primary branches. These authors have observed that small differences in the solidification thermal parameters do not affect significantly the primary dendrite arm spacing. Instead, it has been noted that the primary dendritic arm spacing is more affected by the fluid flow generated due to solute rejection. This is caused by density change on the liquid ahead the solid/liquid interface.

* Corresponding author.
E-mail address: brito87@fem.unicamp.br (C. Brito)

http://dx.doi.org/10.1016/j.ctmat.2016.05.004

Spinelli *et al.* [6] have observed a decrease in the primary dendritic arm spacing of Sn-Pb hypoeutectic alloys in conditions of downward vertical solidification as compared with those grown vertically upwards for the same cooling rate. This effect was attributed to the induced fluid flow, with the heavier solute-enriched melt flowing downwards into the bulk liquid. It appears that this aids the solute rejection and the need for lateral segregation. These authors reported a reduction of about 2.5 times in the primary dendrite arm spacing during downward growth for a same cooling rate. Al-Si hypoeutectic alloys have also been solidified under downward and upward vertical conditions. It was reported that the secondary and the tertiary dendritic arm spacing were not affected significantly by the interdendritic convection [8].

Wang *et al.* [9] have reported recently the importance of density profile ahead the solid/liquid interface. They have investigated the influence of downward and upward directional vertical solidification on the microstructure of CMSX-4 super alloys in order to find a mechanism to avoid freckles caused by density inversion.

In the case of Al-Mg alloys, molten Mg is less dense than Al. Under such conditions, during downward growth, the lighter Mg-enriched interdendritic liquid tends to flow upward and fill the interdendritic spaces. In the upward growth, the Mg-rich melt tends to flow into the bulk liquid. The Mg rejection seems to have stabilizing (downward) or destabilizing (upward) effects on the density stratification depending on the growth direction.

This work aims to analyse the influence of both downward and upward directions of heat extraction during transient directional solidification of an Al-3wt.%Mg alloy. The solidification thermal parameters (cooling rate and growth rate) and microstructural features of both experimental conditions will be examined. Not only experimental interrelations of dendritic arm spacing (λ) and solidification thermal variables are envisaged but also a comparative analysis between these interrelations with the main predictive dendritic growth models from the literature.

2. Experimental Procedure

A water-cooled directional solidification (DS) setup was used in which the unsteady-state solidification takes place vertically downward and upward, as detailed in previous articles [6,10]. The alloy was melted in situ by radial electrical wiring positioned around a cylindrical stainless steel container. For a melt temperature of about 50°C above the *liquidus* temperature, the electric heaters were disconnected, and the water flow at the bottom of the container was initiated, thus permitting the onset of solidification. The DS experiments were carried out with an Al-3wt.%Mg alloy. In order to determining the cooling rate during solidification, fine type K thermocouples (0.2 mm diameter wire) were placed in the geometrical centre of the cylindrical mould cavity along its length. All the thermocouples were connected by coaxial cables to a data logger interfaced with a computer, capable of automatically record temperature data at a frequency of 5 Hz.

The Kroll's reagent and etching times from 1-3 min were used to reveal the microstructures. The optical microscopy was performed using an Olympus Inverted Metallurgical Microscope (model 41GX). The primary dendritic arm spacing (λ_1) and secondary dendritic arm spacing (λ_2) were respectively measured from the optical images of cross and longitudinal sections of the DS casting. The triangle method [11] was used in order to perform (λ_1) measurements. Further, the intercept method was adopted on longitudinal samples in order to determine (λ_2). At least 30 measurements were performed for each selected position along the length of the castings.

Segregation analysis were carried out by a Fluorescence Spectrometer (FRX), model Shimadzu EDX-720, in order to estimate local average concentrations through an area of 100 mm^2 probe.

3. Results and Discussion

Fig. 1 shows a typical macrostructure of the downward solidified Al-Mg alloy casting. It can be observed that the growth of columnar grains has prevailed along the entire casting length. The macro morphology of the casting solidified vertically upward is also characterized by columnar grains. Typical dendritic morphologies of the downward solidified casting from positions (P) at 10 and 70 mm from the metal/mould interface can be seen in Fig. 1.

Fig. 2 a) shows the cooling curves corresponding to the thermal responses of thermocouples inserted along the length of the castings. Based on the experimental thermal profiles, the growth rate and the cooling rate could be determined. The experimental values from Fig. 2 a) have been used to provide plots of position (P) from the metal/mould interface and the corresponding time (t) of the *liquidus* front passing by each thermocouple. Power functions correlating P and (t) have been obtained: $P = 2.8\ t^{0.7}$ (downward) and $P = 2.75\ t^{0.7}$ (upward). The derivatives of these functions with respect to time gave values for the growth rate (V_L), as shown in Fig. 2 b). The cooling rate ($\dot{T}$) was determined along the castings lengths, for thermal data recorded immediately after the passage of the *liquidus* front by each thermocouple.

The growth rate remains coincident for the two growth directions, and a unique cooling rate profile (Fig. 2 c)) could be adjusted trough the experimental data, indicating that the thermal gradient profile (G_L) ahead the dendrite tips is similar between the experiments, since $\dot{T} = G_L.V_L$.

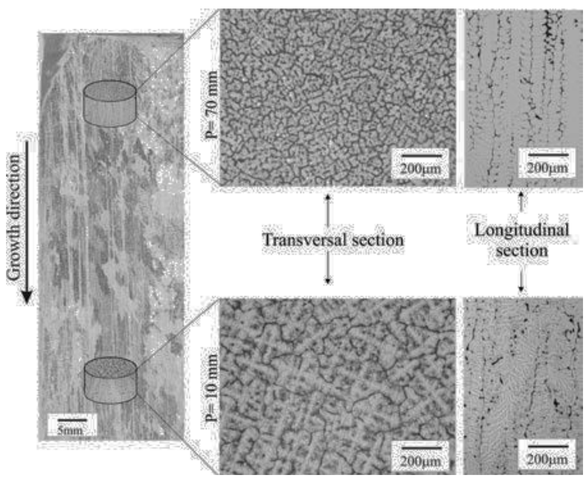

Fig. 1. Macrostructure of the downward solidified Al-3.0wt.%Mg, and some optical microstructures of transverse and longitudinal sections of the casting.

Spinelli *et al.* [12] reported that the heat transfer efficiency at the metal/mould interface is clearly dependent on the orientation of solidification with respect to the gravity vector in downward and upward solidification. It was found that, for the upward configuration, the metal/mould heat transfer efficiency is higher as compared with that of the downward one for a same alloy, since the effect of gravity causes the casting to rest on the mould surface, thus favoring the thermal contact. In contrast, during downward solidification, this action causes the solidified portion of the casting to retreat from the mould surface, and an air gap is formed, increasing the metal/mould thermal resistance. The aforementioned heat transfer behaviour seems not to be present in this study. Analyzing the three cooling curves at about P = 2, 20 and 52 mm for both configurations (Fig. 2 a)), it can be realized that they evolve quite similarly in both upward and downward conditions until the end of solidification at the *solidus* temperature. This fact justifies why the same experimental profiles of growth rate and cooling rate (Figs. 2 b) and c), respectively) reflect either the heat extraction condition of upward or downward solidification. It seems that, during downward solidification, the lighter Mg-rich interdendritic liquid tends to flow upward through the interdendritic channels and possibly could percolate along the dendritic channels reaching the top surface, thus wetting the mould and, in this way, improving the heat extraction. Fig. 3 shows a schematic description of the solute flow from tips to the dendrite roots on the downward condition, and toward the bulk liquid for the upward condition.

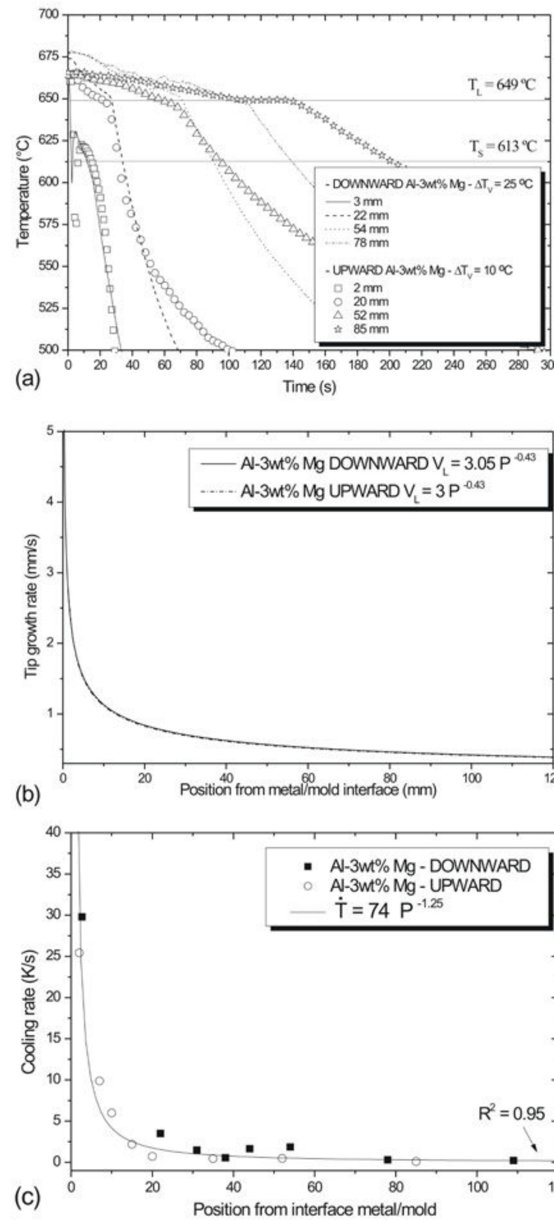

Fig. 2. Experimental cooling curves (a), cooling rate (b), and growth rate (c) for the Al-3wt.%Mg alloy solidified upward and downward. T_L is the *liquidus* temperature, T_S is the *solidus* temperature and ΔT_V is the superheat above T_L.

Fig. 4 presents the average experimental values of primary (λ_1), secondary (λ_2) dendritic arm spacing as a function of cooling rate (primary) and tip growth rate (secondary), respectively, measured from the aforementioned microstructures.

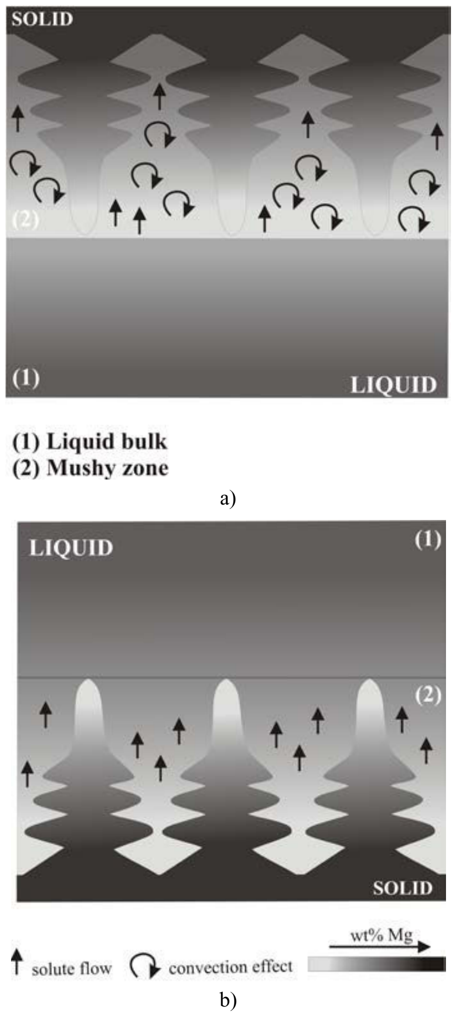

Fig. 3. Schematic representation of solute flow and convection effect along the interdendritic channels: downward (a) and upward (b).

The experimental values of dendritic arm spacing for the upward and downward conditions are quite similar in both cases when correlated with ($\dot{T}$) and (V_L) permitting unique functions to be fitted in both cases. Experimental growth laws have been proposed, permitting the scale of λ_1 and λ_2 as a function of cooling rate and growth rate during solidification to be predicted, as can be observed in Fig. 4. λ_1 has been characterized by a -0.55 exponent against $\dot{T}$, and the -2/3 exponent seems to be appropriate in the experimental power functions relating λ_2 to the growth rate, as shown in Figs. 4 a) and b), respectively. These exponents are the same reported in previous studies with Sn-Pb, Al-Cu and Al-Si alloys [6-8,13] solidified under similar conditions.

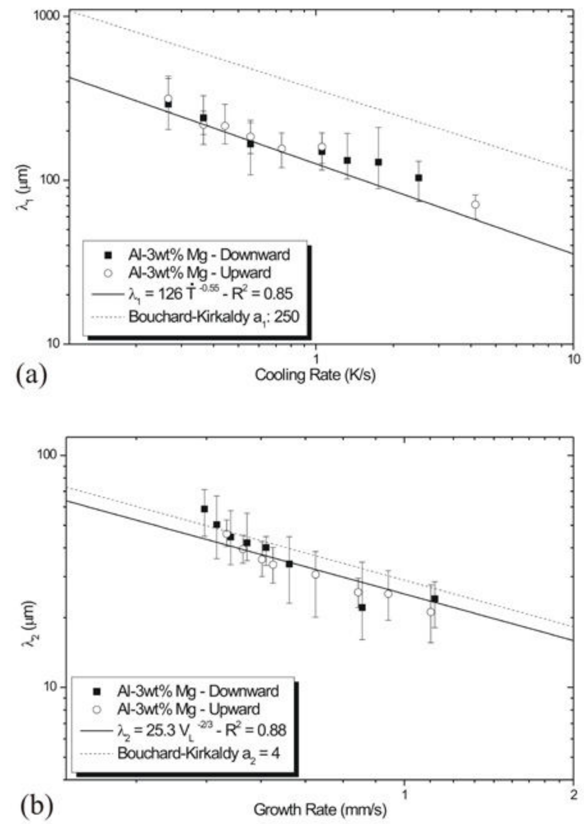

Fig. 4. Correlations between dendrite arm spacing and solidification thermal parameters during solidification of the Al-3.0wt.%Mg in favour (downward growth) and against (upward) gravity vector: λ_1 evolution as a function of cooling rate (a), and λ_2 evolution as a function of growth rate (b).

The figures also show comparisons between the present experimental dendritic arm spacing with theoretical predictions furnished by an unsteady-state predictive model proposed by Bouchard-Kirkaldy (BK) [14], represented by Eqs. (1) and (2).

$$\lambda_1 = a_1 \left(\frac{16 C_0^{1/2} G_0 \varepsilon \Gamma D}{(1-k_0) m_L G_L V_L} \right)^{1/2} \tag{1}$$

where $G_0\varepsilon$ represents a characteristic parameter $\approx$ 600x6 K/cm [14], m_L the slope of the *liquidus* line, k_0 the solute partition coefficient, C_0 the alloy composition, Γ the Gibbs–Thomson coefficient, D the liquid solute diffusivity and a_1 and a_2 the primary and secondary dendrite-calibrating factors, respectively, which depend on the alloy composition and T_F the fusion temperature of the solvent.

$$\lambda_2 = 2\pi a_2 \left(\frac{4\Gamma D}{C_0 (1-k_0)^2 T_F} \left(\frac{D}{V_L} \right)^2 \right)^{1/3} \tag{2}$$

It can be seen that $a_1 = 250$ overestimates the λ_1 experimental scatter, which is an indication that the calibration factor cannot be assumed as a constant for Al alloys, as claimed by BK. Actually, in a previous study on validation of primary dendritic growth models, Spinelli *et al.* [13] reported that the theoretical predictions by the BK model, performed with the originally suggested a_1 factor, overestimate the experimental scatters for Al-Si, Al-Cu, Al-Ni and Al-Sn alloys, and that appropriate a_1 values should be determined for specific binary alloys systems. On the other hand, the calibrating factor ($a_2 = 4$) suggested by BK for Al-Ni alloys, which was adopted in the present work, matches well the λ_2 experimental trend.

The XRF analyses have been carried out in order to evaluate the distribution of Mg along the length of the castings. Additionally, Si and Fe contents were measured as impurities. Mg is expected to be rejected ahead the solid/liquid interface during the progress of solidification since the partition coefficient (k) is lower than 1.0. Furthermore, Mg is less dense than Al. Considering that a Mg-rich liquid will be formed ahead the solidification front, this liquid would tend to flow toward the open liquid in the casting solidified upwards, i.e., in an opposite direction with respect to the gravity vector. In contrast, the volumetric contraction accompanying solidification would tend to induce downward interdendritic flow (through the columnar dendritic channels) of the Mg-enriched melt. This seems to lead to a balance between upward gravity-driven flow and downward shrinkage contributions, thus leading to a resultant stable segregation profile during upward solidification. During downward solidification, the aforementioned effects would act in reverse directions; however, with a similar result. That is, part of the Mg-rich liquid would flow upwards due to the volumetric shrinkage contribution while the solidification front, moving downwards, would carry along part of the less-dense Mg-rich liquid, and again a balance of solute distribution would be met. The main impurities (Si and Fe) seem to be carried along with the aforementioned induced flow in both directions. These situations are experimentally reflected in Fig. 5 by essentially constants profiles of solute as a function of position from the metal/mould interface, which can be roughly represented by horizontal lines.

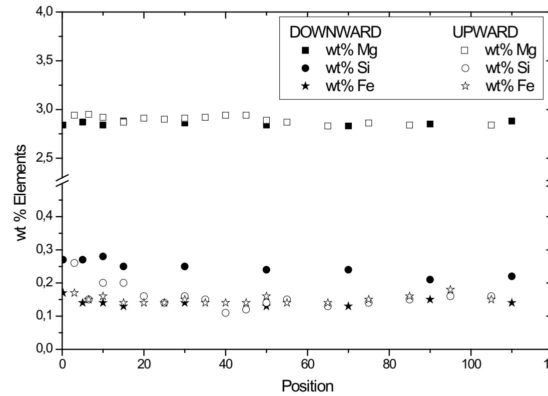

Fig. 5. Macrosegregation profiles for magnesium, silicon and iron along the DS downward and upward casting length.

4. Conclusions

The following major conclusions are derived from the present study:

– Comparing the mean values of λ_1 and λ_2 obtained from the upward vertical experiment with those from the downward one, the dendritic arm spacing are not significantly affected by the interdendritic convection for both solidification directions;

– A -0.55 power law characterizes the $\lambda_1$variation with the cooling rate and a -2/3 power law the λ_2 variation with the growth rate for both upward or downward solidification;

– The Bouchard–Kirkaldy model overestimates the experimental primary dendritic arm spacing. On the other hand, it agrees fairly well with the secondary spacing experimental data.

Acknowledgements

The authors acknowledge the financial support provided by FAPESP – São Paulo Research Foundation, Brazil (Grants 2012/08494-0, 2012/16328-2, 2013/23396-7, 2014/25809-0 and 2014/50502-5) and CNPq (The Brazilian Research Council).

References

[1] M.H. Avazkonandeh-Gharavol, M. Haddad-Sabzevar, H. Fredriksson, J. Alloys Compd. 610 (2014) 462.
[2] E.J. Lavernia, J.D. Ayers, T.S. Srivatsan, Int. Mater. Rev. 37 (1992) 1.
[3] R. Trivedi, J.A. Sekhar, V. Seetharaman, Metall. Trans. A 20A (1989) 769.

[4] W.W. Mullins, R.F. Sekerka, J. Appl. Phys. 35 (1964) 444.
[5] M.H. Burden, J.D. Hunt, Met. Sci. 10 (1976) 156.
[6] J.E. Spinelli, I.L. Ferreira, A. Garcia, J. Alloys Compd. 384 (2004) 217.
[7] J.E. Spinelli, D.M. Rosa, I.L. Ferreira, A. Garcia, J. Mater. Sci. Eng. A 383 (2004) 271.
[8] J.E. Spinelli, M.D. Peres, A. Garcia, J. Alloys Compd. 403 (2005) 228.
[9] F. Wang, D. Ma, J. Zhang, A. Bührig-Polaczek, J. Alloys Compd. 620 (2015) 24.
[10] W.L. Santos, C. Brito, J.M. Quaresma, J.E. Spinelli, A. Garcia, J. Mater. Sci. Eng. B 182 (2014) 29.
[11] M. Gunduz, E. Çardili, J. Mater. Sci. Eng. A 327 (2002) 167.
[12] J.E. Spinelli, I.L. Ferreira, A. Garcia, Struct. Multidisc. Optim. 31 (2006) 241.
[13] J.E. Spinelli, N. Cheung, A. Garcia, Philos. Mag. 91 (2011) 1705.
[14] D. Bouchard, J.S. Kirkaldy, Metall. Mater. Trans. B 28 (1997) 651.